

## Cooperative Assembly of Magic Number $C_{60}$ -Au Complexes

Yang-Chun Xie, Lin Tang, and Quanmin Guo

*School of Physics and Astronomy, University of Birmingham, Birmingham B15 2TT, United Kingdom*  
(Received 21 August 2013; revised manuscript received 11 October 2013; published 28 October 2013)

We report the assembly of magic number  $(C_{60})_m$ - $(Au)_n$  complexes on the Au(111) surface. These complexes have a unique structure consisting of a single atomic layer Au island wrapped by a self-selected number (seven, ten, or twelve) of  $C_{60}$  molecules. The smallest structure consisting of 7  $C_{60}$  molecules and 19 Au atoms, stable up to 400 K, has a preferred orientation on the surface. We propose a globalized metal-organic coordination mechanism for the stability of the  $(C_{60})_m$ - $(Au)_n$  complexes.

DOI: [10.1103/PhysRevLett.111.186101](https://doi.org/10.1103/PhysRevLett.111.186101)

PACS numbers: 81.16.Dn, 68.37.Ef, 62.23.Eg, 64.75.Yz

Self-assembly of supramolecular structures represents the most promising and practical route for bottom-up nanotechnology [1]. During the last decade, there has been a growing level of interest in transferring supramolecular chemistry to solid surfaces [2–4] for a number of reasons. First of all, there is the technological desire for anchoring molecular structures on a substrate for the purpose of device fabrication. Second, in terms of fundamental studies, there are a large number of characterization techniques particularly suitable for analysis of molecules attached to solid surfaces. Among them are scanning tunneling microscopy (STM) and atomic force microscopy, both capable of imaging molecules with atomic resolution and therefore able to provide direct information for correct interpretation of the bonding mechanisms [2,3]. Moreover, the solid surface itself plays a role in the assembly process, providing the opportunity to build supramolecular architectures not viable in liquid.

Assembly of supramolecular structures on solid surfaces is based mostly on the same 3D noncovalent bonding mechanism as that occurring in solution. The building blocks are linked together by either hydrogen bonding [5–10] or through metal-ligand coordination [11–16]. The effects of dipolar interaction [17,18] and the van der Waals interaction have also been investigated [19,20]. Hydrogen bonding and metal-ligand coordination share the common feature, that bonding occurs specifically in between the relevant functional groups and so is directional. The localized nature of directional bonding accounts for the formation of porous networks [2,6,10]. For molecules where the van der Waals force is the only option for bonding, the range of structures that can be achieved becomes very limited because this force tends to drive the molecules into close-packed arrangements. However, a unique property of the vdW force is that it scales with the size of the molecule and is thus expected to play a dominant role in assembly of large and nonplanar molecules. In this work, we investigate the assembly of  $C_{60}$  molecules around a single atomic layer Au island. The  $C_{60}$  molecule is not functionalized, so its interaction with Au is mainly caused by charge transfer from Au, while the

interaction among the  $C_{60}$  molecules themselves has a strong vdW character. We find the formation of magic number  $C_{60}$ -Au hybrid clusters on the surface indicating preferred  $C_{60}$ /Au ratios. This behavior is similar to the metal-organic coordination phenomenon, but without explicit directional C-Au bonding. Instead, each molecule interacts with a group of Au atoms as well as with neighboring molecules. The stable structure is formed as a result of global optimization of the collective  $C_{60}$ -Au coordination. An earlier report by Schaub *et al.* shows the formation of a  $Kr_{12}$ - $Ag_{19}$  “complex” by decoration of step edges of a planar  $Ag_{19}$  cluster with Kr atoms [21]. Moving from Kr to  $C_{60}$ , there is a dramatic increase in the strength of the vdW force. As a result, the  $C_{60}$  molecules are able to influence the structure of the metal island.

The first step in our experiment is to deposit about  $1 \times 10^{13}$  Au atoms onto the  $1 \text{ cm} \times 0.5 \text{ cm}$  sample at 110 K (the minimum temperature reachable with liquid nitrogen cooling) inside an ultrahigh vacuum chamber, creating an array of Au islands pinned at the elbow sites of the herringbone-reconstructed Au(111) (see Supplemental Material [22] for STM images of the gold islands). This is followed by the deposition of  $\sim 4 \times 10^{12}$  of  $C_{60}$  molecules onto the substrate which is maintained at 110 K. The  $C_{60}$  molecules find the existing Au islands via surface diffusion and encapsulate or partially encapsulate the Au islands as shown in Fig. 1(a). The number of molecules at the elbow site ranges from 1 to  $\sim 15$ . The presence of the small Au island at the elbow site is demonstrated by the “open” shape of the  $C_{60}$  trimers, tetramers, pentamers, etc., in contrast to the close-packed structure formed by  $C_{60}$  alone [23]. The sample is then brought gradually to room temperature (RT). STM imaging performed at RT reveals a number of well-defined  $C_{60}$ -Au complex structures. One of the most abundant structures consists of seven close-packed  $C_{60}$  molecules, Fig. 1(b). The  $(C_{60})_7$  clusters in Fig. 1(b) are located at the fcc region next to the bulged elbow site. They all have the same azimuthal orientation with the molecules close packed along one of the  $\langle 11\bar{2} \rangle$  directions. According to the height profile across a cluster shown in Fig. 1(c), the central molecule is taller than the six surrounding molecules

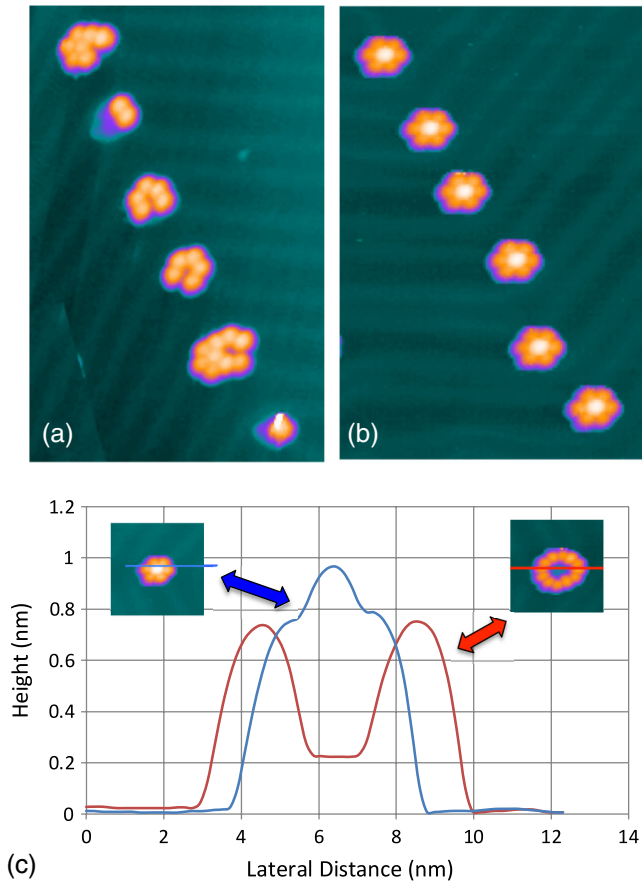


FIG. 1 (color online). (a) STM image ( $25 \text{ nm} \times 40 \text{ nm}$ ) obtained using  $-1.8 \text{ V}$  sample bias and  $0.03 \text{ nA}$  tunnel current showing  $\text{C}_{60}$  molecules aggregating around Au islands at the elbow site at  $110 \text{ K}$ . (b)  $(\text{C}_{60})_7$  clusters with a uniform azimuthal orientation formed at the fcc region next to the bulged elbow site upon temperature rise to RT. The images in (a) and (b) are not from the same location of the sample. (c) Blue curve: height profile across a  $(\text{C}_{60})_7$  cluster. Red curve: height profile across a larger,  $\text{C}_{60}$ -lined Au island.

by  $0.21 \text{ nm}$  which is close to the height of a single atomic step on Au(111). This is clear evidence that the central molecule sits on a single atomic layer Au island and the island itself is encircled by the remaining six molecules. Because the seven molecules inside each cluster are close packed, it points to a unique size, shape, and orientation of the enclosed Au island. There are a small number of circular-shaped Au islands surrounded by  $\text{C}_{60}$  molecules but with no molecule on top of the island. One of them is shown as an inset in Fig. 1(c) together with its height profile. Since the STM has no access to the Au atoms underneath the  $\text{C}_{60}$  molecule, direct counting of the number of Au atoms within each island is not possible. Nevertheless, information from the present work and that of earlier studies [24–30] allows us to propose a model accounting for the most probable and stable structure of the  $\text{C}_{60}$ -Au complex.

Figures 2(a) and 2(b) show the proposed structural model based on a hexagonal Au island consisting of

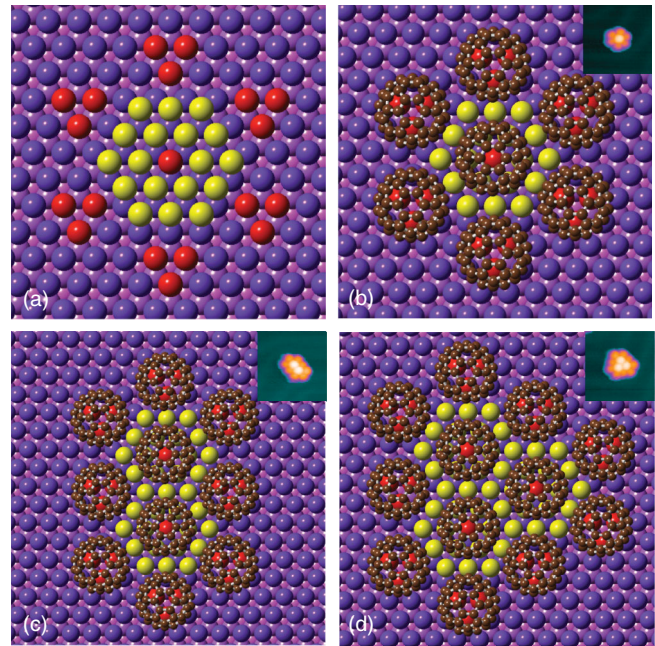


FIG. 2 (color). (a) and (b) Ball model showing the positions of the seven  $\text{C}_{60}$  molecules. Dark purple spheres are the Au atom in the top-most layer of the substrate. Red spheres are top layer Au atoms in direct contact with a hexagonal face of the  $\text{C}_{60}$ . Yellow spheres represent the single atomic layer Au island consisting of 19 Au atoms (c)  $(\text{C}_{60})_{10}$ -Au<sub>35</sub> cluster. Inset is an STM image of such a cluster containing 10  $\text{C}_{60}$  molecules. The two “bright” molecules are sitting side-by-side on top of the gold island. (d)  $(\text{C}_{60})_{12}$ -Au<sub>49</sub> cluster. Inset shows an STM image of such a cluster.

nineteen Au atoms. The six surrounding molecules occupy the threefold fcc hollow site. The central molecule occupies the atop site right at the center of the 19-atom island. As far as the lateral positions of the molecules are concerned, the  $(\text{C}_{60})_7$  cluster takes on exactly the same configuration found within the  $(2\sqrt{3} \times 2\sqrt{3})R30^\circ$  phase of a  $\text{C}_{60}$  monolayer on an extended Au(111) surface [24–28]. The footprint of the central molecule is equivalent to 12 Au atoms, in good agreement with the  $(2\sqrt{3} \times 2\sqrt{3})R30^\circ$  phase of the  $\text{C}_{60}$  monolayer which has one molecule for every twelve surface Au atoms. The distance between the step edge of the 19-atom island and the nearest carbon atom within the  $\text{C}_{60}$  molecule is  $\sim 0.25 \text{ nm}$ , which is very close to the calculated Au-C distance [28] for  $\text{C}_{60}$  on Au(111). This distance depends obviously on whether the molecule is sitting next to a {111}- or a {100}-faceted step, but the difference is very small. Both the height of the molecules and their uniform contrast indicate that the six surrounding molecules are sitting on the surface without involving the atomic vacancy at the interface.

The structural model presented in Figs. 2(a) and 2(b) satisfies the following conditions that are essential for the stability of the  $\text{C}_{60}$ -Au cluster. (i) The optimal distance among the  $\text{C}_{60}$  molecules is maintained for close packing.

Adding an extra Au atom to one side of the 19-atom hexagonal island would force one of the molecules to move sideways and hence weaken the molecule-molecule bonding. (ii) Maximal interaction between the molecules and the Au island is achieved by the proximity of the surrounding molecules to the step edges. It is a known from previous studies that  $C_{60}$  has a strong affinity towards the steps on Au(111) [24,25,29,30]. Removing atoms from the 19-atom cluster would increase the distance between the molecule and the step edge of the island, and hence destabilize the cluster. (iii) The 19-atom Au island is expected to be a magic number supported planar cluster due to its geometrically closed-shell structure [31]. The  $(C_{60})_7$ -Au<sub>19</sub> cluster depicted in Fig. 2(b) derives its stability from the additional interaction between the molecule and the Au island. In fact, bare Au islands of about 19 atoms in size are not stable on Au(111) beyond 200 K. Pure planar  $C_{60}$  clusters containing  $\sim 7$  molecules supported on Au(111) disintegrate when the temperature reaches 240 K [23]. In contrast,  $(C_{60})_7$ -Au<sub>19</sub> clusters like those seen in Fig. 1(b) are stable up to 400 K. The  $C_{60}$  shell acts as a reinforcing layer for the enclosed Au cluster, and the Au cluster in return prevents the molecules from escaping. This type of interaction is similar to metal-ligand coordination [1]. However, the interaction here is not localized between a single metal atom and a specific ligand. Instead, there is expected to be a global optimization process involving all the molecules and the Au atoms within the cluster. As mentioned already, due to the presence of two types of steps of the 19-Au island, the six surrounding molecules are positioned at two slightly different distances from the nearest step edge. This would lead to different bonding strengths of the molecules. Global optimization is able to iron out these differences by allowing atoms and molecules to shift slightly from the predicted positions shown in Fig. 2(a). Furthermore,  $C_{60}$  molecules are not exactly spherical in shape and they have degrees of freedom of tilting or rotating. The molecule on top of the Au island contributes extra stability to the cluster by interacting with all six surrounding molecules through van der Waals bonding.

Using the same approach as that shown in Fig. 2(a), a family of  $(C_{60})_m$ -Au<sub>*n*</sub> clusters can be generated. Fig. 2(c) shows a  $(C_{60})_{10}$ -Au<sub>35</sub> cluster where two  $C_{60}$  molecules are sitting on a Au<sub>35</sub> island. Figure 2(d) shows a  $(C_{60})_{12}$ -Au<sub>49</sub> cluster. Experimentally observed clusters containing ten and twelve  $C_{60}$  molecules are shown as insets in Figs. 2(c) and 2(d), respectively. For the  $(C_{60})_7$ -Au<sub>19</sub> cluster, the six molecules surrounding the Au island are in a similar bonding environment with each molecule interacting with a three-atom long step edge. For the larger hybrid clusters, there are molecules interacting with longer, V-shaped step edges. There are two such molecules in Fig. 2(c) and three in Fig. 2(d). This gives an impression that larger clusters may become more stable. However, as the cluster size increases, the number of molecules sitting on top of the Au island

increases, and these molecules are not as strongly bound to the substrate as the ones sitting at the foot of the step edge. Therefore, the bonding energy per molecule is not necessarily going to increase with the size of the hybrid cluster. This gives rise to the abundance of the  $(C_{60})_7$ -Au<sub>19</sub> cluster on the surface as shown in Fig. 3. In Fig. 3, all the different shaped clusters observed in the experiment are shown. The two circled clusters in the figure are made of  $(C_{60})_7$ -Au<sub>19</sub> plus one extra molecule. The cluster inside the rectangle has six  $C_{60}$  molecules. It has all the features of a  $(C_{60})_7$ -Au<sub>19</sub> cluster but with a missing molecule. The Au island associated with this cluster must have a size and shape very similar to that with the  $(C_{60})_7$ -Au<sub>19</sub> cluster. There is a  $(C_{60})_{14}$  cluster, inside the oval, which can be viewed as a  $(C_{60})_{10}$  cluster such as that shown in Fig. 2(c) plus four extra molecules. In this Letter we will not discuss the less abundant irregular clusters.

The herringbone reconstruction of the Au(111) surface is not lifted in the presence of the  $(C_{60})_m$ -Au<sub>*n*</sub> clusters. The clusters are confined within the fcc region at the elbow sites. The  $(C_{60})_7$ -Au<sub>19</sub> cluster has the right size to be comfortably fitted in between the discommensuration lines. If more molecules are added to the  $(C_{60})_7$ -Au<sub>19</sub> cluster, these extra molecules will have to sit above the discommensuration lines. In fact, for the larger  $(C_{60})_m$ -Au<sub>*n*</sub> clusters, there are always molecules sitting on top of the discommensuration lines. There is plenty of experimental

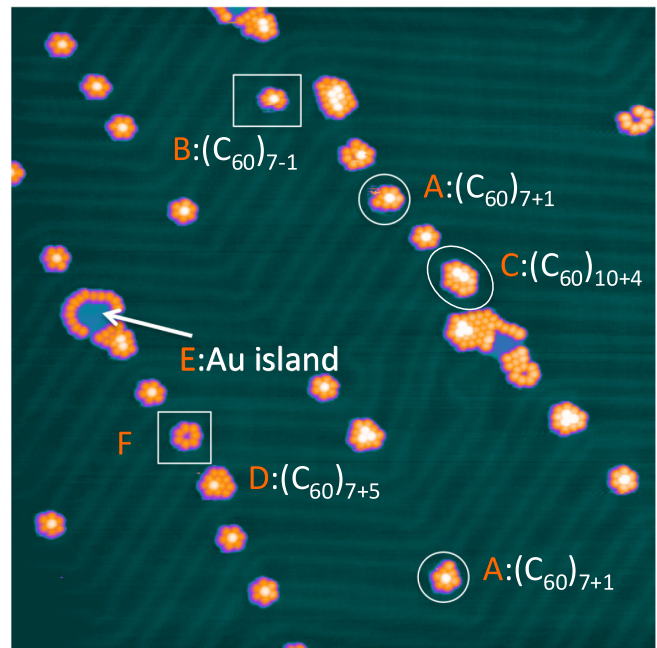


FIG. 3 (color online). Different types of  $(C_{60})_m$ -Au<sub>*n*</sub> complexes. A:  $(C_{60})_7$  cluster with an extra molecule. B:  $(C_{60})_7$  cluster with a missing molecule. C:  $(C_{60})_{10}$  cluster with four additional molecules. D:  $(C_{60})_7$  cluster with extra five molecules. E: A relatively large irregular Au island with its step edges decorated by  $C_{60}$  molecules. F: Seven  $C_{60}$  molecules forming a closed cage around a Au island with no molecule sitting on top of the island.

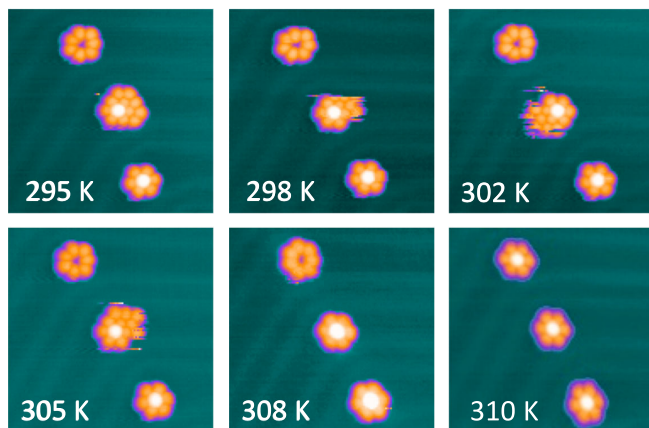


FIG. 4 (color online). Self-refining towards the stable  $(C_{60})_7\text{-Au}_{19}$  cluster. The three clusters are followed continuously as the sample temperature is slowly raised. The whole sequence of image collection takes  $\sim 6$  h. These six images are from a collection of more than 100 images.

evidence that molecules prefer either the fcc [32] or the hcp [33] region of the surface by avoiding the discommensuration lines. Therefore, in the present case, the discommensuration line impedes the  $(C_{60})_7\text{-Au}_{19}$  cluster from capturing more molecules. In a few cases, the  $(C_{60})_7\text{-Au}_{19}$  cluster has been observed to uproot from the elbow site and drift along the fcc region between the discommensuration lines.

Next, we demonstrate the self-refining phenomenon of the hybrid clusters. By self-refining, we mean self-organized transition from metastable to stable configurations under thermal activation. In Fig. 4, three clusters with different initial sizes and shapes are imaged with the STM and their response to slow temperature rises is followed continuously over several hours. The cluster at the bottom of the image is a stable  $(C_{60})_7\text{-Au}_{19}$ , and it does not exhibit any change as the temperature is raised. The cluster at the top of the image consists of seven molecules around a Au island forming a ringlike structure. The Au island here is larger than  $\text{Au}_{19}$  because seven molecules can be fitted along its boundary. One of the seven  $C_{60}$  molecules manages to jump up to the top of the Au island at 310 K, and with the re-organization of the remaining six molecules they form a new  $(C_{60})_7\text{-Au}_{19}$  cluster. A number of Au atoms may have been released from the island in the above re-organizational process. The exchange of  $C_{60}$  molecules and gold atoms on the surface facilitates the ripening of the magic-number clusters. In the middle of the image there is a  $(C_{60})_{12}$  cluster consisting of a stable  $(C_{60})_7\text{-Au}_{19}$  cluster as the core with five peripheral molecules. These five peripheral molecules are seen to wander around the edges of the stable core until they are detached at 308 K leaving behind a stable  $(C_{60})_7\text{-Au}_{19}$  cluster. At 310 K, we see three clusters with the same size, shape, orientation, and likely the same chemical composition. Further increase in temperature has no effect on these three stable clusters until they are fragmented at about 400 K.

The above analysis shows a clear thermally activated self-refining capability of the  $(C_{60})_m\text{-Au}_n$  clusters. Such a self-refining process removes unstable structures, promotes the transition from metastable structures to stable structures. Structures similar to  $(C_{60})_7\text{-Au}_{19}$  have been produced previously by depositing Au atoms onto a uniform  $C_{60}$  monolayer on Au(111) [34,35]. In that case, deposited Au atoms manage to pass through the molecular layer to the interface. The atoms then aggregate at the interface into single layer Au island which is inserted between the  $C_{60}$  molecule and the Au(111) substrate. Producing size-selected nanostructures with well-defined shapes and composition has attracted a great deal of attention. A number of interesting  $C_{60}$ -based structures have been successfully realized in the past using the template effect of the supporting substrate [36–39]. Our approach described here adds a new dimension to the already explored field of supramolecular nanostructures.

In conclusion, magic number  $(C_{60})_m\text{-Au}_n$  hybrid clusters are synthesized on the Au(111) surface. These clusters are stabilized by a metal-ligand type of coordination where a globalized optimization of molecule-metal and molecule-molecule interactions is achieved. The clusters possess a self-refinement capability by simultaneously fulfilling size-, orientation-, and composition selection. The process developed can be used, for example, to fabricate magnetic quantum dot arrays for spin applications, by using either magnetic seeding islands or single molecule magnets or a combination of both. To narrow down the size distribution even further, one can choose to deposit size-selected Au clusters [40] such as  $\text{Au}_{19}$  as the seed. The magic number hybrid clusters reported here should not be restricted to  $C_{60}\text{-Au}$ . Other molecule-metal combinations are expected to produce similar complexes when the size and shape of the metal island fulfill the requirements of the molecule.

This work was supported by the Engineering and Physical Sciences Research Council of the United Kingdom. Y.-C. X. thanks the University of Birmingham for an MPAGS studentship.

- 
- [1] R. Chakrabarty, P. S. Mukherjee, and P. J. Stang, *Chem. Rev.* **111**, 6810 (2011).
  - [2] J. V. Barth, *Annu. Rev. Phys. Chem.* **58**, 375 (2007).
  - [3] J. A. A. Elemans, S. Lei, and S. De Feyter, *Angew. Chem., Int. Ed.* **48**, 7298 (2009).
  - [4] F. Rosei, M. Schnack, Y. Naitosh, P. Jiang, A. Gourdon, E. Lagsgaard, I. Stensgaard, C. Joachim, and F. Besenbacher, *Prog. Surf. Sci.* **71**, 95 (2003).
  - [5] A. Dimitriev, N. Lin, J. Weckesser, J. V. Barth, and K. Kern, *J. Phys. Chem.* **106**, 6907 (2002).
  - [6] J. A. Theobald, N. S. Oxtoby, M. A. Phillips, N. R. Champness, and P. H. Beton, *Nature (London)* **424**, 1029 (2003).

- [7] A. Ciesielski, P.J. Szabelski, W. Rzyzsko, A. Cadeddu, T.R. Cook, P.J. Stang, and P. Samori, *J. Am. Chem. Soc.* **135**, 6942 (2013).
- [8] L.-A. Fendt, M. Stohr, N. Wintjes, M. Enache, T.A. Jung, and F. Diederich, *Chem. Eur. J.* **15**, 11 139 (2009).
- [9] A.D. Jewell, S.M. Simpson, A. Enders, E. Zurek, and E.C.H. Sykes, *J. Phys. Chem. Lett.* **3**, 2069 (2012).
- [10] G. Pawin, K.-L. Wong, K.-Y. Kwon, and L. Bartels, *Science* **313**, 961 (2006).
- [11] M. Pivetta, G.E. Pacchioni, U. Schlickum, J.V. Barth, and H. Brune, *Phys. Rev. Lett.* **110**, 086102 (2013).
- [12] H.-H. Yang, Y.-H. Chu, C.-I. Lu, T.-H. Yang, K.-J. Yang, C.-C. Kaun, G. Hoffmann, and M.-T. Lin, *ACS Nano* **7**, 2814 (2013).
- [13] J. Mendez, R. Caillard, G. Otero, N. Nicoara, and J.A. Martin-Gago, *Adv. Mater.* **18**, 2048 (2006).
- [14] F. Hanke, S. Haq, R. Raval, and M. Persson, *ACS Nano* **5**, 9093 (2011).
- [15] F. Klappenberger, D. Kuhne, W. Krenner, I. Silanes, A. Arnau, F.J. Garcia de Abajo, S. Klyatskaya, M. Ruben, and J.V. Barth, *Phys. Rev. Lett.* **106**, 026802 (2011).
- [16] D. Ecija, J.I. Urgel, A.C. Papageorgiu, S. Joshi, W. Auwärter, A.P. Seitsonen, S. Klyatskaya, M. Ruben, S. Fischer, S. Vijayaraghavan, J. Reichert, and J.V. Barth, *Proc. Natl. Acad. Sci. U.S.A.* **110**, 6678 (2013).
- [17] F. Bischoff, K. Seufert, W. Auwärter, S. Joshi, S. Vijayaraghavan, D. Ecija, K. Diller, A.C. Papageorgiu, S. Fischer, F. Allegretti, D.A. Ducan, F. Klappenberger, F. Blobner, R. Han, and J.V. Barth, *ACS Nano* **7**, 3139 (2013).
- [18] I. Fernandez-Torrente, S. Monturet, K.J. Franke, J. Fraxedas, N. Lorente, and J.I. Pascual, *Phys. Rev. Lett.* **99**, 176103 (2007).
- [19] T. Chen, G.B. Pan, H. Wettach, M. Fritzsche, S. Hoger, L.J. Wan, H.B. Yang, B.H. Northrop, and P.J. Stang, *J. Am. Chem. Soc.* **132**, 1328 (2010).
- [20] D. De Boer, M. Krikorian, B. Esser, and T.M. Swager, *J. Phys. Chem. C* **117**, 8290 (2013).
- [21] R. Schaub, H. Jodicke, F. Brunet, R. Monot, J. Buttet, and W. Harbich, *Phys. Rev. Lett.* **86**, 3590 (2001).
- [22] See Supplemental Material at <http://link.aps.org/supplemental/10.1103/PhysRevLett.111.186101> for details of experimental methods and analysis of cluster size distribution.
- [23] X. Zhang, L. Tang, and Q. Guo, *J. Phys. Chem. C* **114**, 6433 (2010).
- [24] E.I. Altman and R.J. Cotton, *Surf. Sci.* **279**, 49 (1992).
- [25] X. Zhang, F. Yin, R.E. Palmer, and Q. Guo, *Surf. Sci.* **602**, 885 (2008).
- [26] L. Tang, Y.-C. Xie, and Q. Guo, *J. Chem. Phys.* **135**, 114702 (2011).
- [27] J.A. Gardener, G.A. D. Briggs, and M.R. Castell, *Phys. Rev. B* **80**, 235434 (2009).
- [28] X. Torrelles, M. Pedio, C. Cepek, and R. Felici, *Phys. Rev. B* **86**, 075461 (2012).
- [29] L. Tang, X. Zhang, and Q. Guo, *Surf. Sci.* **604**, 1310 (2010).
- [30] L. Tang, X. Zhang, and Q. Guo, *Langmuir* **26**, 4860 (2010).
- [31] Y.-P. Chiu, L.-W. Huang, C.-M. Wei, C.-S. Chang, and T.-T. Tsong, *Phys. Rev. Lett.* **97**, 165504 (2006).
- [32] M. Bohringer, K. Morgenstern, W.D. Schneider, R. Berndt, F. Mauri, A. DeVita, and R. Car, *Phys. Rev. Lett.* **83**, 324 (1999).
- [33] M. Pivetta, M.-C. Blum, F. Patthey, and W.-D. Schneider, *Chem. Phys. Chem* **11**, 1558 (2010).
- [34] L. Tang, Y.-C. Xie, and Q. Guo, *J. Chem. Phys.* **136**, 214706 (2012).
- [35] Y.-C. Xie, L. Tang, and Q. Guo, *J. Phys. Chem. C* **116**, 5103 (2012).
- [36] L. Sanchez, R. Otero, J.M. Gallego, R. Miranda, and N. Martin, *Chem. Rev.* **109**, 2081 (2009).
- [37] W. Xiao, P. Ruffieux, K. Ait-Mansour, O. Groning, K. Palotas, W.A. Hofer, P. Groning, and R. Fasel, *J. Phys. Chem. B* **110**, 21 394 (2006).
- [38] K. Ait-Mansour, P. Ruffieux, W. Xiao, P. Groning, R. Fasel, and O. Groning, *Phys. Rev. B* **74**, 195418 (2006).
- [39] D.V. Gruznev, A.V. Matetskly, L.V. Bondarenko, O.A. Utas, A.V. Zotov, A.A. Saranin, J.P. Chou, C.M. Wei, M.Y. Lai, and Y.L. Wang, *Nat. Commun.* **4**, 1679 (2013).
- [40] Z.W. Wang and R.E. Palmer, *Nano Lett.* **12**, 5510 (2012).